

Bootstrapping the Chiral Anomaly at Large N_c

Teng Ma^{1,2}, Alex Pomarol^{1,3} and Francesco Sciotti¹

¹*IFAE and BIST, Universitat Autònoma de Barcelona, 08193 Bellaterra, Barcelona*

²*ICTP-AP, University of Chinese Academy of Sciences, 100190 Beijing, China*

³*Departament de Física, Universitat Autònoma de Barcelona, 08193 Bellaterra, Barcelona*

Abstract

The bootstrap approach (demanding consistency conditions to scattering amplitudes) has shown to be quite powerful to tightly constrain gauge theories at large N_c . We extend previous analysis to scattering amplitudes involving pions and external gauge bosons. These amplitudes allow us to access the chiral anomaly and connect low-energy physical quantities to UV properties of the theory. In particular, we are able to obtain an analytic bound on the chiral anomaly coefficient as a function of the pion dipole polarizabilities. This bound can be useful for holographic models whose dual UV completions are not known, and provide a consistency condition to lattice simulations.

1 Introduction

In the large- N_c limit strongly-coupled gauge theories find a dual description as weakly-coupled theories of mesons and glueballs [1, 2]. This has allowed to obtain valuable information on QCD in the strongly-coupled regime. In spite of this, the fact that the theory contains infinite number of states with all spins has made difficult to get quantitative predictions on physical quantities.

Recently [3, 4], it has been shown that a better quantitative understanding of large- N_c theories can be achieved by requiring consistency conditions, such as unitarity and causality, to the scattering amplitudes [5–13]. Thanks to the simple analytical structure of the scattering amplitudes at large- N_c , positivity constraints have provided precise and strong bounds on low-energy quantities, such as Wilson coefficients of the chiral Lagrangian as well as meson couplings. High-spin states contributions to these low-energy physical quantities have shown to be small, giving an understanding of the phenomenological successes of Vector Meson Dominance and holographic QCD [4].

We extend these previous analysis to scattering amplitudes of Goldstones (π and η) interacting with external gauge bosons (W). The main purpose is to access information related to the chiral anomaly and other physical quantities such as pion polarizabilities. In particular, we will analyze the amplitudes $W\pi \rightarrow W\pi$ and $W\pi \rightarrow \eta\pi$, this later being proportional, at low-energies, to the chiral anomaly. We will understand the meson exchange selection rules that apply to these amplitudes and that will help us to derive the sign of their on-shell residues. By demanding a good high-energy behaviour of the scattering amplitudes, we will derive dispersion relations that will allow us to obtain interesting bounds on low-energy quantities.¹

Our main result will be the derivation of an upper bound on the coefficient of the chiral anomaly κ :

$$\frac{\kappa}{\sqrt{\mathcal{P}/F_\pi^2}} \leq \sqrt{\frac{1}{2}}, \quad (1)$$

where F_π is the pion decay constant, and \mathcal{P} , to be specified later, is related to pion polarizabilities. This bound provides a non-trivial connection between low-energy physical quantities and UV properties of the theories.² On the other hand, for phenomenological models for QCD, such as a holographic or NJL models, the above upper bound can provide a valuable consistency check, as well as for lattice simulations.

The analysis described here can also be useful to derive constraints on a large number of low-energy physical constants, specially to those related to the electromagnetic properties of pions and other mesons.

The paper is organized as follows. In Sec. 2 we discuss the properties of amplitudes for pions and gauge bosons and derive the dispersion relations and null constraints. In Sec. 3, we analytically derive an upper bound on the chiral anomaly coefficient. We conclude in Sec. 4. The appendices contain details about the classification of mesons and the signs of residues (A), pion polarizabilities (B), numerical bounds on Wilson coefficients (C), and su -models (D).

¹Previous studies in the context of QCD can be found in [14–22].

²Bounds on the a -anomaly from scattering amplitudes requirements have been derived in [23, 24].

2 Amplitudes for pions and external gauge bosons in the large- N_c limit

We are interested in studying $SU(N_c)$ gauge theories in the large- N_c limit. We will consider that the theory also contains N_f massless quarks (q_L, q_R) in the fundamental representation of $SU(N_c)$, with the following pattern of chiral symmetry breaking: $U(N_f)_L \times U(N_f)_R \rightarrow SU(N_f) \times U(1)$. The massless Goldstone bosons associated with the breaking of this global symmetry are the pions (π^a with $a = 1, \dots, N_f^2 - 1$ in the adjoint representation of $SU(N_f)$) and the η (singlet). The chiral axial symmetry $U(1)_A$ is anomalous but in the large- N_c limit the corresponding Goldstone, the η , remains massless.

As usual, we will introduce the coupling to external gauge bosons by gauging the global $SU(N_f) \times U(1)$ symmetry. These gauge bosons will be considered (non-propagating) external fields, sitting in the adjoint and singlet representations.

For simplicity, we will concentrate in this paper in the $N_f = 2$ case, but the arguments we make can be extended straightforwardly to a general N_f . For $N_f = 2$ the pions and gauge bosons are isospin triplets, π^a and W^a , and isospin singlets, the η and B .³ We are interested in the following amplitudes:

(a)

(b)

(c)

(2)

The amplitude (a) is important as, at low-energies, becomes proportional to the chiral anomaly coefficient that we want to bootstrap. For this purpose, as we will see, we will also need the amplitudes (b) and (c). The amplitude (c) was already discussed in detail in [3, 4]. In this section we will then only discuss the amplitudes (b) and (a) in the large- N_c limit for the different polarizations of the gauge bosons $\lambda_W = \pm 1$. In the following, we will derive the relevant dispersion relations necessary to obtain sum rules for the chiral anomaly coefficient and other Wilson coefficients, as well as null constraints necessary for obtaining bounds.

2.1 Exchanged meson states

In the large- N_c limit, a $SU(N_c)$ gauge theory reduces to a theory of weakly-coupled mesons, whose trilinear couplings scale as $\sim 1/\sqrt{N_c}$ [1, 2]. Amplitudes are then mediated by tree-level meson exchange. In the amplitudes (2), the exchanged mesons are colorless $q\bar{q}$ states that, as in the quark model, can be classified according to their quantum numbers: Isospin (I), G -parity (G), parity (P) and spin (J). The relation between these quantum numbers is discussed in Appendix A.⁴ We have six types of mesons as shown in Table 1. It is important to say that in

³We normalize the gauge bosons as $W^a T^a + B \mathbb{I}/2$, where $\text{Tr}[T^a T^b] = 1/2$, and the gauge coupling $g = 1$.

⁴Fixing I , G and P , the spin J is fixed to either be even or odd, as explicitly shown in Table 1.

	Isospin $I = 0$	Isospin $I = 1$		n
$G = +1$	$J_{\text{odd}}^+ (f_J)$	$J_{\text{odd}}^+ (a_J)$	$G = -1$	1
	$J_{\text{even}}^+ (f_J)$	$J_{\text{even}}^+ (a_J)$		2
	$J_{\text{even}}^- (\eta_J)$	$J_{\text{even}}^- (\pi_J)$		3
$G = -1$	$J_{\text{odd}}^+ (h_J)$	$J_{\text{odd}}^+ (b_J)$	$G = +1$	4
	$J_{\text{odd}}^- (\omega_J)$	$J_{\text{odd}}^- (\rho_J)$		5
	$J_{\text{even}}^- (\omega_J)$	$J_{\text{even}}^- (\rho_J)$		6

Table 1: List of $q\bar{q}$ states classified in terms of their Isospin, G -parity and J^P . We also provide the names as they are generally referred to in QCD [25]. In green we highlight the states that enter in the amplitude $W\pi \rightarrow \eta\pi$ which is related to the chiral anomaly.

the large- N_c limit, each $I = 1$ state (left column) has an $I = 0$ associated state (the one next in the right column) of equal mass and related couplings due to the underlying $U(2)$ symmetry [1, 2].

2.2 The $\pi W \rightarrow \pi W$ Amplitudes

Let us start with the amplitude (b). For $N_f = 2$, the most general structure we can write for this amplitude takes the form

$$\mathcal{M}(W^a, \pi^b, W^c, \pi^d) = A_t(s, u)\delta_t + \tilde{A}(s, u)\delta_s + \tilde{A}(u, s)\delta_u, \quad (3)$$

where $s = (p_a + p_b)^2$, $t = (p_a - p_c)^2$, $u = (p_a - p_d)^2$, and $\delta_s = \delta_{ab}\delta_{cd}$, $\delta_t = \delta_{ac}\delta_{bd}$, $\delta_u = \delta_{ad}\delta_{cb}$. We have demanded the amplitude to be invariant under the exchange of the two pions that also requires $A_t(s, u)$ to be $s \leftrightarrow u$ symmetric.

In the large- N_c limit this amplitude is mediated by tree-level exchanges of mesons, either in the s -channel, t -channel and/or u -channel. Since $q\bar{q}$ states cannot have $I = 2$, it will be important to focus in $I = 2$ eigen-amplitudes. These are given by

$$M_s^{I=2} = A_t(s, u) + \tilde{A}(u, s), \quad M_t^{I=2} = \tilde{A}(s, u) + \tilde{A}(u, s), \quad M_u^{I=2} = A_t(s, u) + \tilde{A}(s, u), \quad (4)$$

respectively for the s , t and u -channel. These amplitudes cannot have mesons exchanging in the s , t and u -channel respectively.

In the amplitude Eq. (3) the s -channel and u -channel exchanged meson i couples to $W\pi$,

while the t -channel exchanged meson couples to WW and $W\pi$:

$$\begin{array}{ccc}
\begin{array}{c} W \quad W \\ \diagdown \quad \diagup \\ \bullet \text{---} \bullet \\ \diagup \quad \diagdown \\ \pi \quad \pi \end{array} & \propto g_{W\pi i}^2 &
\begin{array}{c} W \quad W \\ \diagdown \quad \diagup \\ \bullet \text{---} \bullet \\ \diagup \quad \diagdown \\ \pi \quad \pi \end{array} & \propto g_{W\pi i}^2 &
\begin{array}{c} W \quad W \\ \diagdown \quad \diagup \\ \bullet \text{---} \bullet \\ \diagup \quad \diagdown \\ \pi \quad \pi \end{array} & \propto g_{WWi} g_{\pi\pi i} \end{array} \quad (5)$$

Since the couplings g_{WWi} do not appear in the amplitude $W\pi\eta\pi$ (the one related to the chiral anomaly), we will restrict to situations in which the t -channel meson exchange is not present such that we will not have to deal with these couplings g_{WWi} any longer. This can be achieved by either taking t -fixed or working with $M_t^{I=2}$. This leaves only 3 possibilities to consider:

1. $M_t^{I=2}$ at u -fixed,
2. $M_t^{I=2}$ at t -fixed,
3. $M_u^{I=2}$ at t -fixed.

Notice that we have not included $M_s^{I=2}$ since it contains the same information as $M_u^{I=2}$ as far as our positivity arguments are concerned.

It is also of central importance to understand the sign of the on-shell couplings of the meson being exchanged, or, equivalently, the sign of the residues at the mass poles. Defining these as $R_{I=1,0}$ for the $I = 1, 0$ mesons respectively, we have

$$\begin{array}{l}
\mathcal{M}(\delta_t \neq 0, \delta_s = \delta_u = 0) = A_t(s, u) \xrightarrow[\text{onshell}]{s\text{-channel}} \begin{array}{c} W^b \quad W^b \\ \diagdown \quad \diagup \\ \bullet \text{---} \bullet \\ \diagup \quad \diagdown \\ \pi^a \quad \pi^a \end{array} = - \sum_i \frac{(R_{I=1})_i}{s - m_i^2}, \\
\mathcal{M}(\delta_s \neq 0, \delta_t = \delta_u = 0) = \tilde{A}(s, u) \xrightarrow[\text{onshell}]{s\text{-channel}} \begin{array}{c} W^b \quad W^a \\ \diagdown \quad \diagup \\ \bullet \text{---} \bullet \\ \diagup \quad \diagdown \\ \pi^b \quad \pi^a \end{array} = - \sum_i \frac{(R_{I=0})_i}{s - m_i^2},
\end{array}$$

where the sum over i runs over all the possible intermediate states. Knowing that the amplitudes Eq. (4) cannot have poles at the s , t and u -channel respectively, we can derive the relative sign of the residues in the s and u -channel, which we show in Table 2.

For $I = 1(0)$ mesons, we have 3 types of states, $n = 1, 2, 3(4, 5, 6)$, given in Table 1. The signs of their residues depend on the helicity of the external vector states. We have two independent possibilities, either an elastic process ($W^+\pi \rightarrow W^+\pi$) which we will refer to as the $+-$ amplitude, or inelastic ($W^+\pi \rightarrow W^-\pi$) which we will refer to as the $++$ amplitude. Following the discussion of Appendix A, one finds that the signs of the residues are given by

$$\begin{array}{ll}
R_{I=0}^{+-} = +g_4^2 + g_5^2 + g_6^2 & R_{I=1}^{+-} = +g_1^2 + g_2^2 + g_3^2, \\
R_{I=0}^{++} = -g_4^2 + g_5^2 - g_6^2 & R_{I=1}^{++} = -g_1^2 + g_2^2 - g_3^2, \end{array} \quad (6)$$

Meson channel	$-A_t(s, u)$	$-\tilde{A}(s, u)$	$-\tilde{A}(u, s)$
s -channel	$R_{I=1}$	$R_{I=0}$	$-R_{I=1}$
u -channel	$R_{I=1}$	$-R_{I=1}$	$R_{I=0}$

Table 2: Residues in the s and u -channel of the amplitudes A_t and \tilde{A} .

where we have defined

$$g_n^2 \equiv g_{\pi W, n}^2 > 0, \quad n = 1, \dots, 6, \quad (7)$$

and n labels the different type of mesons as defined in Table 1.

The helicity configuration forces a particular kinematic pre-factor in the amplitude which, in the spinor helicity formalism, can be written as

$$\mathcal{M}^{+-} \propto \langle 12 \rangle^2 [23]^2 \propto su, \quad \mathcal{M}^{++} \propto [13]^2 \propto s + u, \quad (8)$$

where the numbers label the states as in Fig. 2 (b).

At energies below the mass M of the lightest massive meson, we can expand the amplitudes in powers of $s/M, u/M \rightarrow 0$. For the elastic scattering amplitude we have

$$\begin{aligned} M_t^{I=2}(s, u)|_{+-} &= 2 + su \left(\sum_{m=0}^{\infty} \sum_{l=0}^{[m/2]} g_{m,l} s^{\{m-l\}} u^l \right) \\ &= 2 + su (g_{0,0} + g_{1,0} (s + u) + g_{2,0} (s^2 + u^2) + 2g_{2,1} su + \dots), \end{aligned} \quad (9)$$

$$\begin{aligned} M_u^{I=2}(s, u)|_{+-} &= -1 - su \left(\sum_{m=0}^{\infty} \sum_{l=0}^{[m/2]} h_{m,l}^s s^{\{m-l\}} u^l + \sum_{m=0}^{\infty} \sum_{l=0}^{[m/2]} h_{m,l}^a s^{\{m-l\}} u^l \right) \\ &= -1 - su (h_{0,0}^s + h_{1,0}^s (s + u) + h_{1,0}^a (s - u) + h_{2,0}^s (s^2 + u^2) + \dots), \end{aligned} \quad (10)$$

where Eq. (9) is fully $s \leftrightarrow u$ symmetric, and in Eq. (10) we have separated the symmetric and the antisymmetric part. The first terms of the expansion correspond to the pion exchange whose gauge coupling we normalize to 1. On the other hand, for the inelastic scattering amplitude we have

$$\begin{aligned} M_t^{I=2}(s, u)|_{++} &= (s + u) \left(\sum_{m=0}^{\infty} \sum_{l=0}^{[m/2]} f_{m,l} s^{\{m-l\}} u^l \right) \\ &= (s + u) (f_{0,0} + f_{1,0} (s + u) + f_{2,0} (s^2 + u^2) + f_{2,1} su + \dots). \end{aligned} \quad (11)$$

We do not need to give the expression for the low-energy expansion of $M_u^{I=2}(s, u)|_{++}$ since, as we will see, this amplitude does not provide any extra information for bounding the chiral anomaly. The low-energy constants $g_{m,l}$, $h_{m,l}^s$, $h_{m,l}^a$ and $f_{m,l}$, referred here as Wilson coefficients, are the low-energy parameters that we want to constrain.

2.3 Dispersion Relations and Null Constraints

In order to derive sum rules and null constraints from our dispersion relations, we will assume that for all $k \geq k_{\min}$, the amplitudes behave as follows at high energies (k_{\min} will be indicated for the various processes):

$$\lim_{|s| \rightarrow \infty} \frac{M_t^{I=2}(s, u)}{s^k} \rightarrow 0, \quad (12a) \qquad \lim_{|s| \rightarrow \infty} \frac{M_t^{I=2}(s, -t - s)}{s^k} \rightarrow 0, \quad (12b)$$

$$\lim_{|s| \rightarrow \infty} \frac{M_u^{I=2}(s, -s - t)}{s^k} \rightarrow 0. \quad (12c)$$

The amplitudes can be expanded in partial waves in the physical regions. For the elastic process we have

$$\begin{aligned} \text{Im} M_{u,t}^{I=2}(s, u)|_{+-} &= \sum_i (2J+1) \rho_J^{+-,\pm}(s) d_{1,1}^J(\cos \theta_s), \\ (2J+1) \rho_J^{+-,\pm}(s) &= \pi \sum_i \left(R_{I=0}^{+-} \pm R_{I=1}^{+-} \right)_i m_i^2 \delta(s - m_i^2) \delta_{JJ_i}, \end{aligned} \quad (13)$$

where the u, t subscript refers to the \pm spectral density and $\cos \theta_s = (t - u)/s$. For the inelastic amplitude similarly we have

$$\begin{aligned} \text{Im} M_{u,t}^{I=2}(s, u)|_{++} &= \sum_i (2J+1) \rho_J^{++,\pm}(s) d_{1,-1}^J(\cos \theta_s), \\ (2J+1) \rho_J^{++,\pm}(s) &= \pi \sum_i \left(R_{I=0}^{++} \pm R_{I=1}^{++} \right)_i m_i^2 \delta(s - m_i^2) \delta_{JJ_i}. \end{aligned} \quad (14)$$

2.3.1 Elastic Process

For the elastic process the dispersion relations that we will consider involve $M_t^{I=2}$ at fixed $u < 0$ and fixed $t < 0$, and $M_u^{I=2}$ at fixed $t < 0$ (all in the s -plane). The analytic structure of these amplitudes and the contours we choose for the dispersion relations can be found in Fig. 1. For the elastic process we define the high-energy average along the lines of [11] as

$$\langle (\dots) \rangle_{+-}^{\pm} \equiv \frac{1}{\pi} \sum_i (2J+1) \int_{M^2}^{\infty} \frac{dm^2}{m^2} \rho_J^{+-,\pm}(m^2) (\dots). \quad (15)$$

- $M_t^{I=2}$ u -fixed:

The integral of $M_t^{I=2}(s, u)/s^{k+1}$ along the contour C_{∞} of Fig. 1a vanishes for $k \geq k_{\min}$, due to Eq. (12a). Because of the amplitude's analyticity, we can deform C_{∞} into the blue contour in Fig. 1a giving

$$\oint_{C_0} ds' \frac{M_t^{I=2}(s', u)}{s'^{k+1}} = 2i \int_{M^2}^{\infty} ds' \frac{\text{Im} M_t^{I=2}(s', u)}{s'^{k+1}}. \quad (16)$$

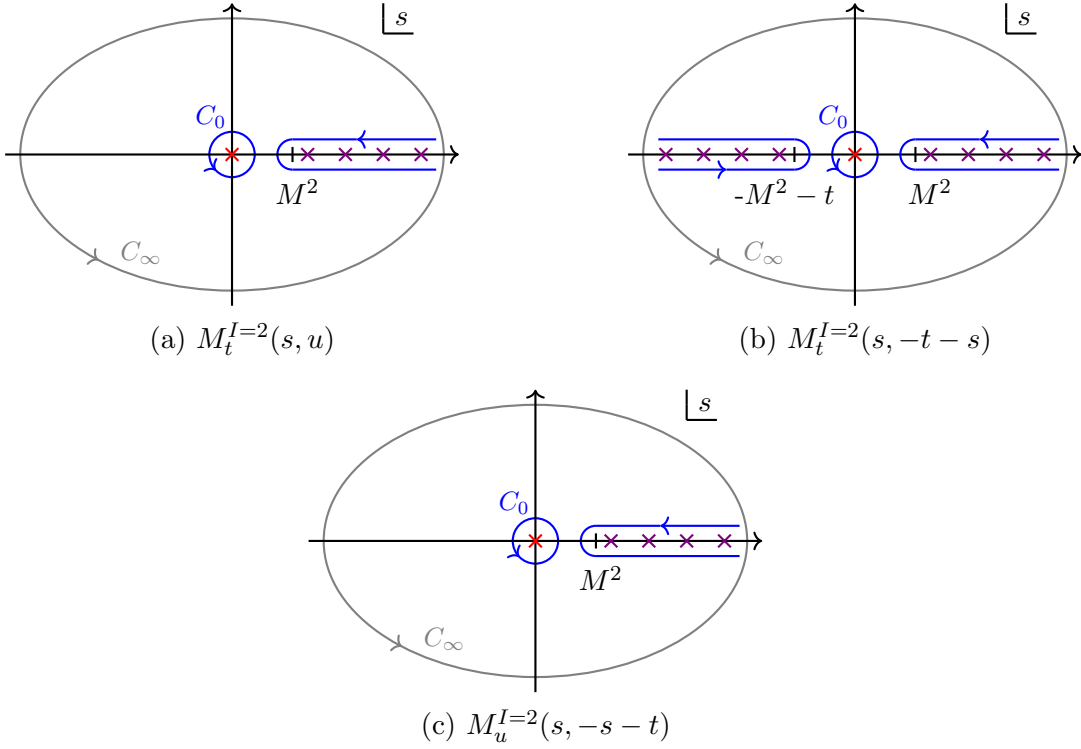


Figure 1: Analytic structure of $M_t^{I=2}$ at fixed $u < 0$ (a), fixed $t < 0$ (b) and of $M_u^{I=2}$ at fixed $t < 0$ (c). We denote by C_0 , C_∞ (to be taken at $|s| \rightarrow \infty$) and the discontinuity along the real axis the relevant contours of integration used for the dispersion relations.

Assuming $k_{\min} = 1$, we are able to derive, inserting Eq. (13) into Eq. (16) and expanding for $u \rightarrow 0$, the following system of relations:

$$\begin{aligned}
(k=1) \quad g_{0,0}u + g_{1,0}u^2 + \dots &= \left\langle \frac{(-1)^J \mathcal{J}^2}{2m^4} u + \frac{(-1)^J \mathcal{J}^4}{6m^6} u^2 + \dots \right\rangle_{+-}^-, \\
(k=2) \quad g_{1,0}u + g_{2,1}u^2 + \dots &= \left\langle \frac{(-1)^J \mathcal{J}^2}{2m^6} u + \frac{(-1)^J \mathcal{J}^4}{6m^8} u^2 + \dots \right\rangle_{+-}^-, \\
&\vdots
\end{aligned} \tag{17}$$

where $\mathcal{J}^2 = J(J+1)$, $\mathcal{J}^4 = (J-1)J(J+1)(J+2)$, etc... . The system above allows us to relate the low-energy Wilson coefficients to the high-energy UV-averages:

$$g_{0,0} = \left\langle \frac{(-1)^J \mathcal{J}^2}{2m^4} \right\rangle_{+-}^-, \quad g_{1,0} = \left\langle \frac{(-1)^J \mathcal{J}^2}{2m^6} \right\rangle_{+-}^-, \quad \dots \tag{18}$$

Furthermore one can notice that the system is over-constrained and therefore it is possible to find a set of non trivial null constraints, the first of which starts at $\mathcal{O}(1/m^6)$:

$$\left\langle \frac{(-1)^J \mathcal{J}^2}{2m^6} \right\rangle_{+-}^- = \left\langle \frac{(-1)^J \mathcal{J}^4}{6m^6} \right\rangle_{+-}^-. \tag{19}$$

Nevertheless, as we will show later, the null constraints needed to bound the chiral anomaly are only those at $\mathcal{O}(1/m^4)$.

- $M_t^{I=2}$ t -fixed:

We can repeat the arguments explained above for $M_t^{I=2}(s, -s - t)$ at fixed $t < 0$. The integral identity one gets using Cauchy's theorem, following Fig. 1b, is

$$\frac{1}{2i} \oint_{C_0} ds' \frac{M_t^{I=2}(s', -t - s')}{s'^{k+1}} = \int_{M^2}^{\infty} ds' \frac{\text{Im} M_t^{I=2}(s', -t - s')}{s'^{k+1}} + (-1)^k \int_{M^2}^{\infty} ds' \frac{\text{Im} M_t^{I=2}(s', -t - s')}{(s' + t)^{k+1}}. \quad (20)$$

This dispersion relation leads to a system of equations ⁵

$$(k = 2) \quad -g_{0,0} + g_{1,0}t + \dots = \left\langle \frac{2}{m^4} \right\rangle_{+-}^- + \left\langle \frac{2\mathcal{J}^2 - 5}{m^6} \right\rangle_{+-}^- t + \dots, \quad (21)$$

$$\vdots$$

that is not over-constrained. Therefore, by themselves, these equations do not lead to any null constraint. Nevertheless, we can combine it with the u -fixed system in Eq. (17) to get a new set of null constraints. We will be interested in the one at $\mathcal{O}(1/m^4)$ which we will need to constrain the anomaly. This is given by

$$\left\langle \frac{(-1)^J \mathcal{J}^2 + 4}{2m^4} \right\rangle_{+-}^- = 0. \quad (22)$$

Notice that the averages are taken with $R_{I=0}^{+-} - R_{I=1}^{+-}$, and therefore positivity is not guaranteed.

- $M_u^{I=2}$ t -fixed:

The amplitude $M_u^{I=2} = A_t(s, u) + \tilde{A}(s, u)$ at t -fixed is the only one whose residues are all positive, as can be seen from Table 2. It has poles only in the s -channel, as can be seen in Fig. 1c. According to Eq. (13) the high-energy average will now have a positive spectral density $\rho_J^{+-,+}(s) > 0$. The dispersion relations look identical to Eq. (16), but with the low-energy amplitude given by Eq. (10). Following the steps explained in the previous sections, we can find sum rules for the Wilson coefficients of Eq. (10), as for example (for $k = 2$),

$$h_{0,0}^s = \left\langle \frac{1}{m^4} \right\rangle_{+-}^+. \quad (23)$$

The conditions one gets from these dispersion relations (analogous to Eq. (17)) is however not over-constrained, and therefore no additional null constraints are obtained.

⁵We can assume here $k_{\min} = 2$ as $k = 1$ does not provide additional information.

2.3.2 Inelastic Process

Let us now focus on the inelastic process. In particular, out of the three possible dispersion relations listed in Fig. 1, we will only consider $M_t^{I=2}$ at fixed $u < 0$ and fixed $t < 0$ in the s -plane.⁶ We can proceed similarly as in the previous sections, but with the low-energy amplitude given in Eq. (11), the partial-wave decomposition given in Eq. (14), and the high-energy average defined by

$$\langle (\dots) \rangle_{++}^{\pm} \equiv \frac{1}{\pi} \sum_i (2J+1) \int_{M^2}^{\infty} \frac{dm^2}{m^2} \rho_J^{++,\pm}(m^2) (\dots). \quad (24)$$

- $M_t^{I=2}$ u -fixed:

Once again the integral of $M_t^{I=2}(s, u)/s^{k+1}$ along the contour C_{∞} of Fig. 1a vanishes for $k \geq k_{\min}$, due to Eq. (12a). We have again Eq. (16) that expanded for small u gives

$$\begin{aligned} (k=1) \quad f_{0,0} + 2f_{1,0}u + \dots &= \left\langle \frac{(-1)^{J+1}}{m^2} - \frac{(-1)^J(J^2 + J - 1)}{m^4} u + \dots \right\rangle_{++}^{-}, \\ (k=2) \quad f_{1,0} + (f_{2,1} + f_{2,0})u + \dots &= \left\langle \frac{(-1)^{J+1}}{m^4} - \frac{(-1)^J(J^2 + J - 1)}{m^6} u + \dots \right\rangle_{++}^{-}, \\ &\vdots \end{aligned} \quad (25)$$

leading to a new set of null constraints. At $\mathcal{O}(1/m^4)$, we have

$$\left\langle \frac{(-1)^J(\mathcal{J}^2 - 3)}{2m^4} \right\rangle_{++}^{-} = 0. \quad (26)$$

- $M_t^{I=2}$ t -fixed:

For fixed $t < 0$, we can obtain new dispersion relations that combined with the system Eq. (25) leads to a second set of null constraints. By doing this, one can notice that the first new null constraint enters at order $\mathcal{O}(1/m^6)$.

2.3.3 Bounds on Wilson coefficients

From the above dispersion relations it is already possible to obtain interesting bounds on the low-energy Wilson coefficients of the $W\pi W\pi$ amplitude, that are related to physical quantities such as the dipole and quadrupole polarizabilities of the pions (see Appendix B). A more detailed discussion is given in Appendix C. For example, at $\mathcal{O}(s^2)$, we find the bounds

$$-2 \leq \frac{g_{0,0}}{h_{0,0}^s} \leq 2, \quad -1 \leq \frac{f_{1,0}}{h_{0,0}^s} \leq 1. \quad (27)$$

For higher-order Wilson coefficients a numerical analysis is sometimes needed in order to find the allowed values. In Figure 2 we provide an example (see Appendix C for details).

⁶We will not consider $M_u^{I=2}$ in the inelastic case. The corresponding dispersion relations were only useful for the elastic case to relate Wilson coefficients, such as $h_{0,0}^s$, to sums over positive residues.

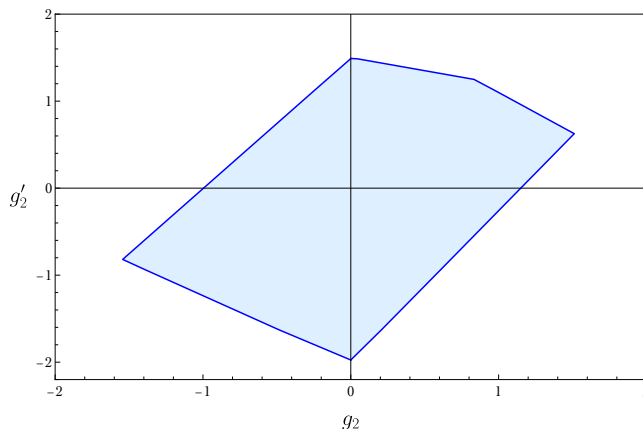


Figure 2: *Exclusion plot for the Wilsons g_2 and g'_2 given in Eq. (62).*

2.4 The $W\pi \rightarrow \eta\pi$ Amplitude and the Chiral Anomaly

Let us now consider the $W\pi \rightarrow \eta\pi$ amplitude. For $\lambda_W = +1$ helicity, we have

$$\mathcal{M}(W^{a+}, \pi^b, \eta, \pi^c) \propto [12]\langle 24 \rangle [41] \propto \sqrt{stu}. \quad (28)$$

At low-energy, this amplitude can be written as

$$|\mathcal{M}(W^{a+}, \pi^b, \eta, \pi^c)| = |f_{abc}| \mathcal{M}_{W\pi\eta\pi} = \frac{\kappa}{2\sqrt{2}} |f_{abc}| \sqrt{stu} + \dots \quad (29)$$

The Wilson coefficient κ is related to the chiral anomaly. Indeed, from the WZW term [26, 27] we have

$$-\frac{N_c}{48\pi^2} \varepsilon^{\mu\nu\alpha\beta} \text{Tr} [A_{\mu L} U_{\nu L} U_{\alpha L} U_{\beta L} + \text{L} \rightarrow \text{R}] \subset \mathcal{L}_{WZW}, \quad (30)$$

where $U_{\nu L} = (\partial_\nu U)U^\dagger$, $U_{\nu R} = U^\dagger(\partial_\nu U)$, and $U = \text{Exp}(i\eta/F_\pi)\text{Exp}(2i\pi^a\tau^a/F_\pi)$ with $\tau^a = \sigma^a/2$ and $A_L^a = A_R^a = W^a$. By matching Eq. (29) with Eq. (30), we obtain

$$\kappa = \frac{N_c}{12\pi^2 F_\pi^3}. \quad (31)$$

The $W\pi\eta\pi$ amplitude is mediated by the following meson states:

$$\begin{array}{cc}
s/u \text{ - channel:} & \begin{array}{c} W \\ \text{---} I=1 \\ \bullet \text{---} \bullet \\ \text{---} G=-1 \\ \pi \quad \quad \pi \end{array} & t \text{ - channel:} & \begin{array}{c} W \\ \text{---} G=1 \\ \bullet \text{---} \bullet \\ \text{---} I=1 \\ \pi \quad \quad \pi \end{array}
\end{array} \quad (32)$$

For the s/u -channel the exchanged mesons must have $G = -1$, $I = 1$, $J = \text{even}$ and parity $P = (-1)^J = +1$. These states are classified as $n = 2$ in Table. 1 (highlighted in green). On the other hand, in the t -channel the states must have $G = +1$, $I = 1$, $J = \text{odd}$ and $P = (-1)^J = -1$. These states are classified as $n = 5$ in Table. 1 (also highlighted in green). We notice therefore that in this amplitude, only 2 out of the 6 possible types of mesons contribute.

2.5 Dispersion Relations

Let us consider the $W\pi\eta\pi$ amplitude without the non-analytical pre-factor coming from the polarization structure, $\mathcal{M}_{W\pi\eta\pi}/\sqrt{stu}$, and assume at fixed $u < 0$

$$\lim_{|s|\rightarrow\infty} \frac{\mathcal{M}_{W\pi\eta\pi}}{\sqrt{stu}} = 0, \quad (33)$$

and similarly at fixed $t < 0$. In the s -plane with u fixed, we get the following dispersion relation:

$$\oint \frac{ds}{2\pi i} \frac{\mathcal{M}_{W\pi\eta\pi}(s, u)}{\sqrt{-s(s+u)u}} = \sum_i^{J_{\text{even}}^+} \frac{g_{W\pi i} g_{\pi\eta i} d_{1,0}^J(-1 - \frac{2u}{m_i^2})}{\sqrt{-m_i^2(m_i^2 + u)u}} + \sum_i^{J_{\text{odd}}^-} \frac{g_{W\eta i} g_{\pi\pi i} d_{1,0}^J(-1 - \frac{2u}{m_i^2})}{\sqrt{-m_i^2(m_i^2 + u)u}}, \quad (34)$$

where we specified that only J^P mesons with J odd or even are summed over. Expanding the above dispersion relation for $u \rightarrow 0$, we obtain

$$\frac{\kappa}{2\sqrt{2}} = \sum_i^{J_{\text{odd}}^-} \frac{g_{W\eta i} g_{\pi\pi i} \mathcal{J}}{m_i^3} - \sum_i^{J_{\text{even}}^+} \frac{g_{W\pi i} g_{\pi\eta i} \mathcal{J}}{m_i^3}, \quad (35)$$

where $\mathcal{J} = \sqrt{\mathcal{J}^2}$.

Similarly, we can also get another dispersion relation by fixing $t < 0$ in the s -plane. We obtain in this case

$$\frac{\kappa}{2\sqrt{2}} = 2 \sum_i^{J_{\text{even}}^+} \frac{g_{W\pi i} g_{\pi\eta i} \mathcal{J}}{m_i^3}. \quad (36)$$

From Eq. (35) and Eq. (36) we get the null constraint

$$\sum_i^{J_{\text{odd}}^-} \frac{g_{W\eta i} g_{\pi\pi i} \mathcal{J}}{m_i^3} = 3 \sum_i^{J_{\text{even}}^+} \frac{g_{W\pi i} g_{\pi\eta i} \mathcal{J}}{m_i^3}. \quad (37)$$

At large N_c , the couplings of singlet η can be related with the π^a couplings:

$$g_{W\eta i} = (g_5)_i \quad (J_{\text{odd}}^-) \quad , \quad g_{\pi\eta i} = g_{\pi\pi i} \quad (J_{\text{even}}^+). \quad (38)$$

Using these relations, we can express κ and the null constraint Eq. (37) as

$$\frac{\kappa}{4\sqrt{2}} = \sum_i^{J_{\text{even}}^+} \frac{(g_2 g_{\pi\pi})_i \mathcal{J}}{m_i^3} \quad (39)$$

$$= \sum_i^{J_{\text{odd}}^-} \frac{(g_5 g_{\pi\pi})_i \mathcal{J}}{3m_i^3}. \quad (40)$$

3 Bounding the Chiral Anomaly

In this section we analytically derive an upper bound on the anomaly coefficient κ using the $W\pi \rightarrow W\pi$ null constraints Eq. (22) and Eq. (26). These two null constraints are enough to get a bound on κ . We will however improve the bound by incorporating the null constraint Eq. (37) from $W\pi \rightarrow \eta\pi$.

Using the identity (for $a_i, b_i \in \mathbb{R}$)

$$\sum_i a_i b_i \leq \sqrt{\sum_i a_i^2 b_i^2} \leq \sqrt{\left(\sum_i a_i^2\right)\left(\sum_i b_i^2\right)}, \quad (41)$$

we can obtain a bound on κ using Eq. (39) and Eq. (40) respectively

$$\begin{aligned} \frac{\kappa}{4\sqrt{2}} &\leq \sqrt{\left(\sum_i^{J_{\text{even}}^+} \frac{g_{\pi\pi i}^2}{m_i^2}\right)\left\langle\frac{\mathcal{J}^2}{m^4}\right\rangle_2} \equiv \kappa_2^{\text{UB}}, \\ \frac{\kappa}{4\sqrt{2}} &\leq \frac{1}{3}\sqrt{\left(\sum_i^{J_{\text{odd}}^-} \frac{g_{\pi\pi i}^2}{m_i^2}\right)\left\langle\frac{\mathcal{J}^2}{m^4}\right\rangle_5} \equiv \kappa_5^{\text{UB}}. \end{aligned} \quad (42)$$

where we have defined

$$\langle(\dots)\rangle_n \equiv \frac{1}{\pi} \sum_i (2J+1) \int_{M^2}^{\infty} \frac{dm^2}{m^2} \rho_J^n(m^2) (\dots), \quad (43)$$

with

$$(2J+1)\rho_J^n(m^2) = \pi \sum_i (g_n^2)_i m_i^2 \delta(m^2 - m_i^2) \delta_{JJ_i}, \quad (44)$$

and $g_n^2 \geq 0$ defined in Eq. (7). The bounds Eq. (42) depend on \mathcal{J}^2/m^4 high-energy averages which can be written as a function of $1/m^4$ averages by using the null constraints Eq. (22) and Eq. (26), rewritten as

$$\begin{aligned} +\left\langle\frac{\mathcal{J}^2-4}{m^4}\right\rangle_1 - \left\langle\frac{\mathcal{J}^2+4}{m^4}\right\rangle_2 - \left\langle\frac{\mathcal{J}^2+4}{m^4}\right\rangle_3 - \left\langle\frac{\mathcal{J}^2-4}{m^4}\right\rangle_4 - \left\langle\frac{\mathcal{J}^2-4}{m^4}\right\rangle_5 + \left\langle\frac{\mathcal{J}^2+4}{m^4}\right\rangle_6 &= 0, \\ -\left\langle\frac{\mathcal{J}^2-3}{m^4}\right\rangle_1 - \left\langle\frac{\mathcal{J}^2-3}{m^4}\right\rangle_2 + \left\langle\frac{\mathcal{J}^2-3}{m^4}\right\rangle_3 + \left\langle\frac{\mathcal{J}^2-3}{m^4}\right\rangle_4 - \left\langle\frac{\mathcal{J}^2-3}{m^4}\right\rangle_5 - \left\langle\frac{\mathcal{J}^2-3}{m^4}\right\rangle_6 &= 0. \end{aligned} \quad (45)$$

By summing these two relations we get

$$\left\langle\frac{2\mathcal{J}^2}{m^4}\right\rangle_2 + \left\langle\frac{2\mathcal{J}^2}{m^4}\right\rangle_5 = -\left\langle\frac{1}{m^4}\right\rangle_1 - \left\langle\frac{1}{m^4}\right\rangle_2 - \left\langle\frac{7}{m^4}\right\rangle_3 + \left\langle\frac{1}{m^4}\right\rangle_4 + \left\langle\frac{7}{m^4}\right\rangle_5 + \left\langle\frac{7}{m^4}\right\rangle_6. \quad (46)$$

Eq. (46) gives an interesting relation between the two \mathcal{J}^2/m^4 averages involved in Eq. (42) that allows to find the following relation

$$\left\langle\frac{\mathcal{J}^2}{m^4}\right\rangle_2 + \left\langle\frac{\mathcal{J}^2}{m^4}\right\rangle_5 = 3f_{1,0} - 2g_{0,0} \equiv \mathcal{P} \geq 0, \quad (47)$$

where we have used

$$g_{0,0} = \left\langle \frac{2}{m^4} \right\rangle_1 + \left\langle \frac{2}{m^4} \right\rangle_2 + \left\langle \frac{2}{m^4} \right\rangle_3 - \left\langle \frac{2}{m^4} \right\rangle_4 - \left\langle \frac{2}{m^4} \right\rangle_5 - \left\langle \frac{2}{m^4} \right\rangle_6, \quad (48)$$

$$f_{1,0} = \left\langle \frac{1}{m^4} \right\rangle_1 + \left\langle \frac{1}{m^4} \right\rangle_2 - \left\langle \frac{1}{m^4} \right\rangle_3 - \left\langle \frac{1}{m^4} \right\rangle_4 + \left\langle \frac{1}{m^4} \right\rangle_5 + \left\langle \frac{1}{m^4} \right\rangle_6, \quad (49)$$

obtained from the sum rules Eq. (21) and Eq. (25) respectively.

We can also obtain a relation between the sum over $g_{\pi\pi i}^2/m_i^2$ in Eq. (42) by using sum rules derived from dispersion relations for the $\pi\pi \rightarrow \pi\pi$ process in [3, 4]. In particular, we need

$$F_\pi^{-2} = 2 \left(\sum_i^{J_{\text{even}}^+} \frac{g_{\pi\pi i}^2}{m_i^2} + \sum_i^{J_{\text{odd}}^-} \frac{g_{\pi\pi i}^2}{m_i^2} \right). \quad (50)$$

Armed with Eq. (47) and Eq. (50), we can now obtain a bound on κ as a function of F_π^2 and \mathcal{P} . Defining

$$X \equiv F_\pi^2 \sum_i^{J_{\text{odd}}^-} \frac{g_{\pi\pi i}^2}{m_i^2} \quad \text{and} \quad Y \equiv \frac{1}{\mathcal{P}} \left\langle \frac{\mathcal{J}^2}{m^4} \right\rangle_5, \quad (51)$$

we can rewrite κ_5^{UB} and κ_2^{UB} as

$$\frac{\kappa_5^{\text{UB}}}{\sqrt{\mathcal{P}/F_\pi^2}} = \frac{1}{3} \sqrt{XY}, \quad \frac{\kappa_2^{\text{UB}}}{\sqrt{\mathcal{P}/F_\pi^2}} \leq \sqrt{\left(\frac{1}{2} - X\right) \left(\frac{1}{2} - Y\right)}. \quad (52)$$

Written in this way we notice that as we decrease X and Y to make κ_2^{UB} larger, κ_5^{UB} becomes smaller, and viceversa. Since κ must be smaller than both bounds, the largest value of κ is reached when $\kappa_2^{\text{UB}} = \kappa_5^{\text{UB}}$. This is achieved when

$$\frac{1}{9} XY = \left(\frac{1}{2} - X\right) \left(\frac{1}{2} - Y\right) \quad \rightarrow \quad Y = \frac{X - 1/2}{16X/9 - 1}, \quad (53)$$

that inserted in Eq. (52) gives us κ_5^{UB} as a function of only X that is maximized for $X = 3/8$. This corresponds to $Y = 3/8$, and gives $\kappa_5^{\text{UB}}|_{\text{max}} = 1/8$. Taking this value in Eq. (42), we finally get the following upper bound on the chiral anomaly:

$$\frac{\kappa}{\sqrt{\mathcal{P}/F_\pi^2}} \leq \frac{1}{\sqrt{2}}. \quad (54)$$

This is the main result of the paper. This tells us that the anomaly coefficient is bounded by \mathcal{P} , a quantity related with the polarizabilities of the pions (see Appendix B). Using the constraints Eq. (27), we can write Eq. (54) as a function of other Wilson coefficients. For example, we get that $\mathcal{P} \leq 7h_{0,0}^s$ that leads to

$$\frac{\kappa}{\sqrt{h_{0,0}^s/F_\pi^2}} \leq \sqrt{\frac{7}{2}}. \quad (55)$$

In the case of $SU(N_c)$ gauge theories with N_f quarks, the anomaly coefficient κ is known, and Eq. (54) provides a bound on the Wilson coefficients. For example, using Eq. (31) and $F_\pi \simeq \sqrt{N_c/3} m_\rho/7$ [28], we obtain from Eq. (55)

$$h_{0,0}^s \gtrsim \frac{0.44}{m_\rho^4}. \quad (56)$$

As in [3, 4], it is also interesting to obtain the predictions of different models to the ratio Eq. (54), in order to understand how close these are to the upper bound. For example, in models of only scalars, we have that $h_{0,0}^s$ is zero and then $\kappa = 0$. For su -models (introduced in [11] for the first time, and studied in [3, 4, 12] for four-pion amplitudes), we show in Appendix D that

$$\left. \frac{\kappa}{\sqrt{\mathcal{P}/F_\pi^2}} \right|_{su\text{-model}} \lesssim \frac{0.97}{\sqrt{2}}, \quad (57)$$

which falls within the bound established in Eq. (54), only $\sim 3\%$ away from saturation.

Eq. (54) gives a non-trivial constraint on phenomenological models for QCD, such as NJL or holographic models. For example, in holographic models the chiral anomaly arises from a Chern-Simons (CS) term. When the corresponding dual 4D theory is not known, the CS coefficient cannot be matched to the UV theory and therefore cannot be determined. Eq. (54) provides in this case a bound on the size of the CS term. This could also be useful for models of axions.

4 Conclusions

The analyticity, unitarity and the good high-energy behaviour of scattering amplitudes provide severe constraints on the low-energy physical quantities of gauge theories like QCD. In this work we have studied scattering amplitudes involving external gauge fields and goldstones (π and η) in the large- N_c limit to obtain several new constraints.

Our main result has been to provide an analytical bound on the chiral anomaly, Eq. (54). To derive this bound we have first analyzed the $W\pi \rightarrow W\pi$ amplitude, providing the selection rules for the mesons exchanges, as well as the sign of their on-shell residues. We have considered the elastic ($W^+\pi \rightarrow W^+\pi$) and inelastic ($W^+\pi \rightarrow W^-\pi$) processes, as both are needed to derive $\mathcal{O}(1/m^4)$ null constraints on the meson couplings.⁷ We have also derived sum rules for the Wilson coefficients of these amplitudes. Of especial use has been the sum rule for $h_{0,0}^s$ that has shown to have all its terms positive.

We have later considered the $W\pi \rightarrow \eta\pi$ amplitude, which at low energy yields the chiral anomaly coefficient κ . We have shown, once again via dispersion relations, that there are two different ways to determine κ , implying a non-trivial constraint among the corresponding meson couplings.

Putting all this together, we have been able to derive analytically Eq. (54). This bound has interesting implications for UV completions of these amplitudes, as we have shown for

⁷We have found that adding more null constraints does not improve the bound.

the case of large- N_c QCD. We have also considered su -models (see Appendix D) that seem to almost saturate the bound. We hope that in the future this bound could be tested in lattice simulations. Finally, we have also briefly study the bounds on other Wilson coefficients, showing the EFT-hedron geometry [6] of their allowed parameter space -see for example Fig. 2.

In the future, it could also be interesting to study in more detail which theories saturate these bounds. Similarly, our analysis can be extended to understand implications on composite Higgs models and bounds on dimension six operators such as $H^\dagger H F_{\mu\nu} F^{\mu\nu}$.

Note added: While preparing this article, it was submitted to the archives Ref. [29] that also uses dispersion relations to numerically obtain bounds on the chiral anomaly coefficient.

Acknowledgments

We are very grateful to Francesco Riva and Pyungwon Ko for their valuable insights. This work has been partly supported by the research grants 2021-SGR-00649 and PID2020-115845GB-I00/AEI/10.13039/501100011033.

A $q\bar{q}$ mesons and the sign of on-shell residues

The $q\bar{q}$ mesons can be classified according to their quantum numbers: mass m , spin J , parity P , Isospin I , and G -parity. Defining by ℓ the orbital angular momentum of the $q\bar{q}$ system, $s = 0, 1$ the total spin, and $I = 0, 1$ the isospin, we have

$$\begin{aligned} J &= \ell + s, \dots, \ell - s, \\ P &= (-1)^{\ell+1}, \\ G &= (-1)^{I+\ell+s}. \end{aligned} \tag{58}$$

By taking $\ell = 0, 1, 2, \dots$, we can build the meson list of Table 1. Notice that we have only six types of mesons that we label with $n = 1, \dots, 6$.

To understand the sign of the residues in Eq. (6) arising from meson exchanges in the process $W\pi \rightarrow W\pi$, we proceed in the following way (recalling that the couplings $g_{W\pi i}$ are real):

- For the elastic case $W^+\pi \rightarrow W^+\pi$ (amplitude \mathcal{M}^{+-}), we obviously have that these are proportional to $g_{W\pi i}^2 > 0$ so the sign is always positive.
- For $W^+\pi \rightarrow W^-\pi$ (amplitude \mathcal{M}^{++}) we can consider the process $W^+\pi \rightarrow R_i \rightarrow W^-\pi$ in the forward limit $t \rightarrow 0$. By performing a P transformation and a spacial rotation of 180° degrees, the coupling in $W^+\pi \rightarrow R_i$ can be related to that of $R_i \rightarrow W^-\pi$. Using that $d_{1,0}^J(-\cos\theta) = (-1)^J d_{1,0}^J(\cos\theta)$, we have then that $W^+\pi \rightarrow R_i \rightarrow W^-\pi$ is proportional to $g_{W\pi i}^2 \times (-1)^{J_i} \times P_i$.

This leads to the signs in Eq. (6) for the different type of mesons.

B Polarizabilities of the pions

Given the $\gamma\gamma \rightarrow \pi\pi$ scattering amplitude with the pion exchange subtracted, $\mathcal{M}(\gamma^+, \gamma^\pm, \pi, \pi)$, the pion polarizabilities are defined as the coefficients coming from an expansion in s at fixed $t = m_\pi^2$ [18, 30, 31]:

$$\frac{\alpha}{m_\pi} \mathcal{M}(\gamma^+, \gamma^\pm, \pi, \pi)(s, t = m_\pi^2) = (\alpha_1 \mp \beta_1)_\pi + \frac{s}{12} (\alpha_2 \mp \beta_2)_\pi + \dots \quad (59)$$

In particular, $(\alpha_1 \mp \beta_1)_\pi$ and $(\alpha_2 \mp \beta_2)_\pi$ are respectively the dipole and quadrupole polarizabilities of the pions $\pi = \pi^\pm, \pi^0$. These quantities have been measured experimentally [18, 30, 31] and also analyzed in lattice simulations [32]. In our convention the photon corresponds to the gauging of $Q = T_3 + B/2$, a subgroup of the global $U(2)$, and we must change $s \leftrightarrow t$ in Eq. (59). The dipole polarizabilities receive then contributions from our $g_{0,0}$ and $h_{0,0}^s$ for the $+-$ helicities of the photon (although they are suppressed by m_π^2), and $f_{0,0}$ for the $++$. On the other hand, $f_{1,0}$ contributes to the quadrupole polarizability.

C Bounds on the Elastic $W\pi W\pi$ Wilson coefficients

Let us show here how to bound the parameter space of the Wilson coefficients appearing in Eq. (9) and Eq. (10). We are considering the elastic process since better bounds can be obtained in this case due to positivity. Nevertheless, the same approach can also be used for the inelastic case.

Let us begin with the simplest analytical bound arising from the sum rules of $g_{0,0}$ and $h_{0,0}^s$, Eq. (21) and Eq. (23) respectively, that gives

$$\frac{g_{0,0}}{h_{0,0}^s} = - \frac{\langle \frac{2}{m^4} \rangle_{+-}^-}{\langle \frac{1}{m^4} \rangle_{+-}^+}. \quad (60)$$

The absolute value of this ratio must always be smaller or equal to 2, since the states that enter in $g_{0,0}$ and in $h_{0,0}^s$ are the same, the only difference being that in $h_{0,0}^s$ everything enters additively, while some of these states enter with a minus sign in $g_{0,0}$. The bound will be therefore maximized when the only states exchanged are those who contribute negatively to $g_{0,0}$ (namely states with $n = 1, 2, 3$), while it is minimized when the states that contribute positively are the only ones being exchanged ($n = 4, 5, 6$). This leads to the bound Eq. (27), and similarly for $f_{1,0}$ from its sum rule in Eq. (25).

The same result can be found numerically using SDPB [33]. To find this bound we must initially redefine the Wilson coefficients and null constraints (of both the elastic and inelastic processes) in terms of the high-energy average defined Eq. (43), similarly to what was done in Eq. (45). We can then construct the bootstrap equation

$$h_{0,0}\vec{v}_1 + g_{0,0}\vec{v}_2 + \sum_{n=1..6} \langle \vec{v}_n(m^2, J) \rangle_n = 0, \quad (61)$$

which holds true if $\vec{v}_1 = (1, 0, 0, \dots)$, $\vec{v}_2 = (0, 1, 0, \dots)$ and for an appropriate choice of the vectors $\vec{v}_n(m^2, J)$ (which contain the null constraints). Following canonical the optimization procedure explained in detail in [3, 11, 12], one can bound numerically the Wilson coefficients. In particular, this method can be replicated for higher-order Wilson coefficients. For example, defining

$$g_2 = \frac{g_{2,0}}{h_{2,0}^a + 2h_{2,0}^s + h_{2,1}^s/2} \quad \text{and} \quad g'_2 = \frac{g_{2,1}}{h_{2,0}^a + 2h_{2,0}^s + h_{2,1}^s/2}, \quad (62)$$

where the normalization has been chosen opportunely for positivity arguments as

$$h_{2,0}^a + 2h_{2,0}^s + h_{2,1}^s/2 = \left\langle \frac{(\mathcal{J}^2 - 8)\mathcal{J}^2 + 14}{4m^8} \right\rangle_{+-}^+, \quad (63)$$

we can repeat the numerical procedure and find the exclusion plot shown in Figure 2.

D The su -model

The su -models are defined as those leading to healthy amplitudes with a single mass scale m . They often predict Wilson coefficients at the boundaries of the allowed regions [3, 4, 11, 12]. For the $\pi\pi \rightarrow \pi\pi$ process the su -amplitude was already presented in [4] where it was shown to take the general form

$$\mathcal{M}(s, u) \Big|_{4\pi} = \frac{m^2(s+u) + \lambda su}{(s-m^2)(u-m^2)}, \quad (64)$$

with $-2 \leq \lambda \leq \frac{2\ln 2 - 1}{1 - \ln 2}$. In the limiting case $\lambda = \frac{2\ln 2 - 1}{1 - \ln 2}$, the amplitude Eq. (64) contains no poles associated to $J = 0$ states [4]. In this case, the residues in the s -channel of Eq. (64) are given by

$$g_{\pi\pi i}^2 \Big|_{4\pi} = \{0.78, 0.18, 0.04, \dots\}, \quad (65)$$

and correspond to states of $J^P = 1^-, 2^+, \dots$ respectively ($n = 5$ and $n = 2$ of states $G = 1$ alternating). The amplitude Eq. (64) predicts the Wilson coefficient

$$F_\pi^{-2} = \frac{2}{m^2}. \quad (66)$$

Notice that we have absorbed an overall factor in Eq. (64) into F_π^{-2} .

An su -amplitude for $M_t^{I=2}(s, u) \Big|_{+\pm}$ can also be constructed following the conditions:

- It must have a single mass scale m .
- No t -channel poles.
- It must be proportional to t and su for $++$ and $+-$ amplitudes respectively.
- It must drop as $M_t^{I=2}(s, u)/s \rightarrow 0$ for $|s| \rightarrow \infty$ at t -fixed, and similarly for u -fixed.

The most general amplitude following these criteria takes the form

$$M_t^{I=2}(s, u) \Big|_{++} = -\frac{m^2 t}{(s-m^2)(u-m^2)}, \quad M_t^{I=2}(s, u) \Big|_{+-} = -\alpha \frac{su}{(s-m^2)(u-m^2)}, \quad (67)$$

where α is a constant. The residues of Eq. (67) in the s -channel are

$$R_{J=0}^{++} - R_{J=1}^{++} = \{0.82, -0.15, 0.03, \dots\}, \quad R_{J=0}^{+-} - R_{J=1}^{+-} = \alpha \{0.58, -0.09, 0.02, \dots\}. \quad (68)$$

corresponding to $J = 1, 2, 3, \dots$ states, where for each J_{odd} (J_{even}) they can be of type $n = 1, 4, 5$ ($n = 2, 3, 6$) of Table 1.

From Eq. (67) we obtain

$$f_{1,0} = \frac{1}{m^4}, \quad g_{1,0} = -\frac{\alpha}{m^4} \quad \rightarrow \quad \mathcal{P} = \frac{3 + 2\alpha}{m^4}. \quad (69)$$

Notice that we have absorbed an overall factor in the $++$ amplitude in Eq. (67) into $f_{1,0}$.

According to Eq. (6), we can obtain the couplings g_2^2 and g_5^2 (which are the ones that enter in the anomaly), by adding the two sets of residues of Eq. (68). We obtain

$$g_{W\pi i}^2|_{W^2\pi^2} = \{0.41 + 0.29\alpha, 0.07 + 0.05\alpha, \dots\}, \quad (70)$$

corresponding to $n = 5$ and $n = 2$ states alternating. To have positive $g_{5,2}^2$, we must demand $-1.41 \leq \alpha \leq 1.41$. The value $\alpha = 1.41$ (-1.41) maximizes (minimizes) $g_{5,2}^2$.

Finally, the $W\pi\eta\pi$ amplitude can be constructed with the following conditions:

- Single mass scale m .
- $s \leftrightarrow u$ crossing symmetric.
- Proportional to \sqrt{stu} .
- s/u -channel poles associated only to even-spin states (see Eq. (32)).
- It must drop as $\mathcal{M}_{W\pi\eta\pi}/\sqrt{stu} \rightarrow 0$ for $|s| \rightarrow \infty$ at t -fixed, and similarly for u -fixed.

The most general amplitude one can construct following these conditions is

$$\mathcal{M}_{W\pi\eta\pi} = -\beta m \sqrt{stu} \frac{m^2/2 + t}{(s - m^2)(u - m^2)(t - m^2)}, \quad (71)$$

where $\beta > 0$ is a constant. We obtain the following residues in the s -channel:

$$|g_{W\pi i} g_{\pi\pi i}| = \beta \{0.48, 0.10, 0.02, \dots\}, \quad (72)$$

corresponding to states $n = 5$ and $n = 2$ of Table 1 alternating.

From Eq. (29) and Eq. (71) we get the anomaly coefficient

$$\kappa = \frac{\sqrt{2}\beta}{m^3}. \quad (73)$$

To maximize this value, we must take the largest possible value of β . Nevertheless, this is constrained by the fact that the couplings in Eq. (72) cannot overcome

$$\sqrt{g_{W\pi i}^2|_{W^2\pi^2} g_{\pi\pi i}^2|_{4\pi}} = \{\sqrt{0.32 + 0.23\alpha}, \sqrt{0.01 + 0.01\alpha}, \dots\}, \quad (74)$$

coming from Eq. (65) and Eq. (70), as there can always be more states $n = 5, 2$ (for a given J) in Eq. (64) and Eq. (67) than in Eq. (71) (as this latter requires that the interchanged mesons must have both $g_{W\pi i}$ and $g_{\pi\pi i}$ nonzero). This gives

$$\beta_{\max} = \sqrt{1.37 + 0.97\alpha}. \quad (75)$$

With Eq. (66), Eq. (69), Eq. (73) and Eq. (75), one finds that $\kappa/\sqrt{\mathcal{P}/F_\pi^2}$ is maximized for $\alpha = 1.41$, leading to Eq. (57).

References

- [1] G. 't Hooft, Nucl. Phys. B **72**, 461 (1974).
- [2] E. Witten, Nucl. Phys. B **160**, 57 (1979).
- [3] J. Albert and L. Rastelli, JHEP **08**, 151 (2022), arXiv: 2203.11950.
- [4] C. Fernandez, A. Pomarol, F. Riva, and F. Sciotti, JHEP **06**, 094 (2023), arXiv: 2211.12488.
- [5] A. Adams, N. Arkani-Hamed, S. Dubovsky, A. Nicolis, and R. Rattazzi, JHEP **10**, 014 (2006), arXiv: hep-th/0602178.
- [6] N. Arkani-Hamed, T.-C. Huang, and Y.-T. Huang, JHEP **05**, 259 (2021), arXiv: 2012.15849.
- [7] C. de Rham, S. Melville, A. J. Tolley, and S.-Y. Zhou, Phys. Rev. **D96**, 081702 (2017), arXiv: 1702.06134.
- [8] B. Bellazzini, J. Elias Miró, R. Rattazzi, M. Riembau, and F. Riva, Phys. Rev. D **104**, 036006 (2021), arXiv: 2011.00037.
- [9] A. Sinha and A. Zahed, Phys. Rev. Lett. **126**, 181601 (2021), arXiv: 2012.04877.
- [10] A. J. Tolley, Z.-Y. Wang, and S.-Y. Zhou, JHEP **05**, 255 (2021), arXiv: 2011.02400.
- [11] S. Caron-Huot and V. Van Duong, JHEP **05**, 280 (2021), arXiv: 2011.02957.
- [12] S. Caron-Huot, D. Mazac, L. Rastelli, and D. Simmons-Duffin, JHEP **07**, 110 (2021), arXiv: 2102.08951.
- [13] J. Henriksson, B. McPeak, F. Russo, and A. Vichi, JHEP **06**, 158 (2022), arXiv: 2107.13009.
- [14] M. Gourdin and A. Martin, Nuovo Cimento (1955-1965) **17**, 224 (1960).
- [15] P. Ko, Phys. Rev. D **41**, 1531 (1990).

- [16] J. Gasser, M. A. Ivanov, and M. E. Sainio, Nucl. Phys. B **728**, 31 (2005), arXiv: hep-ph/0506265.
- [17] L. V. Fil'kov and V. L. Kashevarov, Phys. Rev. C **72**, 035211 (2005), arXiv: nucl-th/0505058.
- [18] J. Gasser, M. A. Ivanov, and M. E. Sainio, Nucl. Phys. B **745**, 84 (2006), arXiv: hep-ph/0602234.
- [19] U. Burgi, Nucl. Phys. B **479**, 392 (1996), arXiv: hep-ph/9602429.
- [20] L.-Y. Dai and M. R. Pennington, Phys. Rev. D **94**, 116021 (2016), arXiv: 1611.04441.
- [21] X.-L. Ren, I. Danilkin, and M. Vanderhaeghen, Phys. Rev. D **107**, 054037 (2023), arXiv: 2212.03086.
- [22] F. X. Lee, A. Alexandru, C. Culver, and W. Wilcox (2023), arXiv: 2301.05200.
- [23] D. Karateev, J. Marucha, J. a. Penedones, and B. Sahoo, JHEP **12**, 136 (2022), arXiv: 2204.01786.
- [24] J. K. Marucha (2023), arXiv: 2307.02305.
- [25] R. L. Workman et al. (Particle Data Group), PTEP **2022**, 083C01 (2022).
- [26] J. Wess and B. Zumino, Physics Letters B **37**, 95 (1971), ISSN 0370-2693.
- [27] E. Witten, Nuclear Physics B **223**, 422 (1983), ISSN 0550-3213.
- [28] G. S. Bali, F. Bursa, L. Castagnini, S. Collins, L. Del Debbio, B. Lucini, and M. Panero, JHEP **06**, 071 (2013), arXiv: 1304.4437.
- [29] J. Albert and L. Rastelli (2023), arXiv: 2307.01246.
- [30] I. Guiasu and E. E. Radescu, Annals Phys. **122**, 436 (1979).
- [31] M. Moinester (2022), arXiv: 2205.09954.
- [32] X. Feng, T. Izubuchi, L. Jin, and M. Golterman, PoS **LATTICE2021**, 362 (2022), arXiv: 2201.01396.
- [33] D. Simmons-Duffin, JHEP **06**, 174 (2015), arXiv: 1502.02033.